UV–Visible Light-Trapping Structure of Loosely Packed Submicrometer Silica Sphere for Amorphous Silicon Solar Cells

Wen-Hsien Huang, Jia-Min Shieh, Fu-Ming Pan, Chang-Hong Shen, Yu-Chung Lien, Min-An Tsai, Hao-Chung Kuo, Bau-Tong Dai, and Fu-Liang Yang

***Abstract*—We synthesized a loosely packed submicrometer silica-sphere (LPSS) monolayer at room temperature and used the LPSS monolayer as the frontside light-trapping structure for n-i-p-type amorphous Si (a-Si) solar cells (SCs) to improve photovoltaic characteristics of the cells. The frontside LPSS monolayer plays a role as a UV–visible light scatter and a broadband antireflector; both can greatly improve the photoresponse of the underneath a-Si adsorbed layer. When the filling density of the LPSS layer is optimized to 65%, the enhancement in the photocurrent and conversion efficiency of the 120 °C-fabricated SCs is as high as ∼15% and ∼6.9%, respectively. Accordingly, such an LPSS light-trapping structure boosts efficiency of 120 °C- and 140 °C-fabricated cells to 7.3% and 8.5%, respectively. Since the LPSS structure has a graded refractive index profile, it behaves like a nearly omnidirectional antireflector, enhancing solar efficiency at a very large incident angle of illumination.**

***Index Terms*—Omnidirectional reflector, photoresponse, silica sphere, UV–visible.**

I. Introduction

BECAUSE of its low cost and low process thermal budget, the n-i-p-type amorphous silicon (a-Si) thin-film solar cell (SC) has emerged as a potential technique for flexible photovoltaic applications. A highly stable and efficient a-Si SC requires an absorber layer of low-defect density and high spectrum utilization. Backside light-trapping schemes have been widely demonstrated to maintain adequate solar efficiency using thin absorber layers [1]. However, backside reflectors may suffer some extent from the loss of the light-trapping efficiency due to smooth frontside morphology, which is an inevitable consequence of the deposition of a thick absorber layer on the backside reflector. An a-Si SC with a sophisticated nanostructured backside reflector, such as nanopillars and nanodomes [2], typically has a solar efficiency below 6.5%. The frontside dielectric nanoparticle (NP) scatters have been recently proposed to improve the light-trapping efficiency of SC [3], [4]. The light-trapping behavior of silica spheres is dominated by a waveguide mode which scatters sunlight into a-Si and results in the enhanced light absorption within the SC [5], [6]. The light-trapping mechanism for loosely packed submicrometer silica-sphere (LPSS) monolayer is completely different from plasmonic behavior observed in metal NP-based light-trapping structure [4], [6].

The introduction of dielectric spheres can modify the absorption band of the absorber layer depending on the sphere size and the sphere filling density. Submicrometer-sized scatters can increase the absorption rate of a-Si cell in the UV–visible regime because the scatter size is comparable to the illumination wavelength [5], [6]. Furthermore, like pyramid-structured SnO_2, the submicrometer dielectric sphere creates a graded refractive index profile, which may enhance antireflection of a-Si SC. It has been demonstrated that a closely packed silica-sphere (CPSS) monolayer can improve omnidirectional antireflection characteristics of a-Si SC in the long wavelength regime [7]; the CPSS structure is less effective, however, in the short wavelength regime.

In this work, we synthesized an LPSS monolayer on the low-defect a-Si stacks, which was prepared at 120 °C and 140 °C by high-density inductive-coupled plasma (ICP) deposition [8]. The frontside LPSS monolayer greatly enhances the UV–visible photoresponse of the a-Si cell as a result of the enhancement in light scattering by the submicrometer-sized spheres and the formation of a graded refractive index profile [9] that results in nearly omnidirectional antireflection.

II. Experiments

The n-i-p-type a-Si multilayer (20-nm n-layer/400-nm intrinsic i-layer/12-nm p-layer) was deposited on the SnO_2 : F substrate by high-density ICP technique at substrate temperatures of 120 °C and 140 °C [8]. A contact of 80-nm-thick indium tin oxide (ITO) and a 500-nm-thick Al metal grid were then subsequently deposited on the ICP a-Si mutilayer. The sol–gel method was used to synthesize negatively charged monodispersed submicrometer silica spheres at room temperature. The as-prepared a-Si SC structure was then immersed in a mixture of 3-aminopropyltrimethoxysilane (APTMS) and ethanol;

Manuscript received April 13, 2012; accepted April 20, 2012. Date of publication June 8, 2012; date of current version June 22, 2012. The review of this letter was arranged by Editor O. Manasreh.

W.-H. Huang and F.-M. Pan are with the Department of Materials Science and Engineering, National Chiao Tung University, Hsinchu 30050, Taiwan (e-mail: fmpan@faculty.nctu.edu.tw).

J.-M. Shieh is with the National Nano Device Laboratories, Hsinchu 30078, Taiwan, and also with the Department of Photonics and Institute of Electro-Optical Engineering, National Chiao Tung University, Hsinchu 30050, Taiwan (e-mail: jmshieh@ndl.narl.org.tw).

C.-H. Shen, Y.-C. Lien, B.-T. Dai, and F.-L. Yang are with the National Nano Device Laboratories, Hsinchu 30078, Taiwan.

M.-A. Tsai and H.-C. Kuo are with the Department of Photonics and Institute of Electro-Optical Engineering, National Chiao Tung University, Hsinchu 30050, Taiwan.

Color versions of one or more of the figures in this letter are available online at http://ieeexplore.ieee.org.

Digital Object Identifier 10.1109/LED.2012.2196974

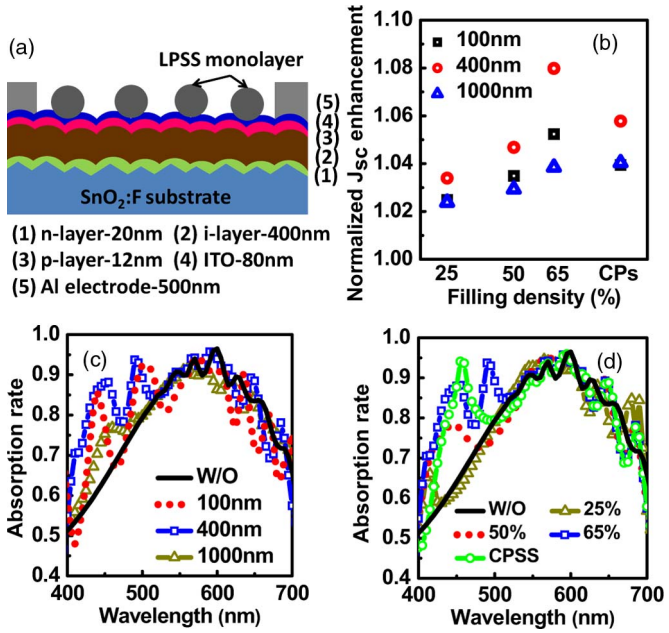

Fig. 1. (a) Schematic structure of the LPSS-capped a-Si SC and (b) simulated normalized $J_{\rm sc}$ as a function of the sphere size and the filling density. The simulated absorption rate of the LPSS monolayer (c) with a filling density of 65% for different sphere sizes and (d) with the 400-nm sphere for different filling densities.

surface damage on the ITO can be avoided by using this method. The APTMS is chemically bonded to ITO and electrostatically attached to silica sphere via the terminal ligand $(-{\rm C}-{\rm NH}_2^+)$, which forms the self-assembly LPSS monolayer on ITO. The angle-dependent reflectance measurement was carried out using a xenon lamp with an illumination angle from $0\,^\circ$ to $80\,^\circ$.

III. Results and Discussion

Fig. 1(a) shows the schematic structure of the a-Si SC with the LPSS light-trapping monolayer. In order to understand the light-trapping of the cell in the UV–visible regime, in which the a-Si exhibits the best quantum efficiency (QE), we first examined the dependence of light absorption on the particle size and the filling density of the LPSS monolayer using the rigorous-coupled-wave-analysis simulation model. The filling density was defined by the volume fraction of silica spheres in the LPSS monolayer; a smaller filling density suggests a larger separation between spheres (hereafter referred to as interspacing).

Fig. 1(b) shows the simulated dependence of the normalized short-circuit current $(J_{\rm sc})$ of the a-Si cell on the particle size and the filling density of the LPSS monolayer. The optimal $J_{\rm sc}$ occurs to the cell with the LPSS layer using 400-nm-sized silica spheres with a filling density of 65%. In contrast, the cell with the LPSS layer using 1000-nm-sized spheres exhibits the smallest $J_{\rm sc}$ for any filling density.

Fig. 1(c) shows the simulated absorption rate of the a-Si cell with an LPSS filling density of 65% for different sphere sizes. The absorption rate in the spectrum range of 400–550 nm increases with the size of the silica sphere as its diameter increases from 100 to 400 nm. However, the absorption rate decreases when the diameter increases to 1000 nm. The increase in UV–visible absorption for the 400-nm sphere

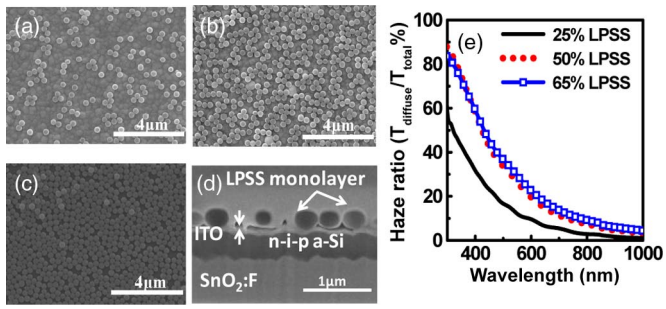

Fig. 2. SEM images of the LPSS monolayer with a filling density of (a) 25%, (b) 65%, and (c) closely packed. (d) Cross-sectional FIB-SEM image of the LPSS-structured a-Si SC. (e) Haze ratio as a function of the light wavelength for the a-Si SC with different LPSS filling densities. The sphere size in the LPSS layer in all the figures is 400 nm.

can be attributed to an enhancement in light scattering in the LPSS monolayer due to the submicrometer-sized dielectric scatter. According to Grandidier's report, enhanced absorption regime for dielectric-sphere-based light-trapping structure is linearly proportional to the sphere diameter due to the optical dispersion relation [6]. Therefore, the silica sphere scatters in LPSS monolayer with the size of 400 nm can increase the absorption rate of the a-Si cell in the UV–visible (400–550 nm) regime.

From Fig. 1(d), the absorption rate of the a-Si cells with 400-nm-sized spheres increases, in terms of the LPSS filling density, in the order $25\% < 50\% < {\rm CPSS} < 65\%$. The combined simulation results of Fig. 1(c) and (d) suggest that an optimal interspacing/diameter (I/D) ratio of the silica sphere in the LPSS monolayer is required to achieve efficient light trapping for the a-Si cell. Kroll *et al.* has shown that light absorption by colloidal monolayer is greatly affected by the I/D ratio of dielectric colloidal spheres [5]. Furthermore, the I/D ratio can also affect the light reflectance of the cell due to the formation of a graded refractive index profile in the LPSS layer. An optimized ratio can result in a significant light trapping in the short wavelength regime. The very low absorption rate of the cell with the filling density of 25% may be ascribed to that light scattering in the LPSS layer is not sufficient to effectively couple into the a-Si absorber or that an ideal graded refractive index profile is absent in the LPSS layer. The simulation results are reasonably in agreement with the experiment results discussed hereinafter.

Fig. 2(a)–(c) shows SEM images of the self-assembly LPSS monolayers. The filling density is controlled from 25% to the closely packed dispersion by adjusting the concentration of APTMS. The focus-ion-beam (FIB)-induced SEM image in Fig. 2(d) shows that the frontside of the a-Si layer has a smoother morphology than the backside. To examine the effect of the filling density on light scattering in the LPSS structure, we measured the haze ratio of the SCs. The haze ratio (H) is defined by $H = T_{\rm diffuse}/T_{\rm total}$, where $T_{\rm diffuse}$ and $T_{\rm total}$ are the diffusive transmittance and the total transmittance, respectively. A higher haze ratio indicates a higher diffusive transmittance, suggesting an increase in the optical path and the photocurrent. Fig. 2(e) shows that the haze ratio is the smallest for a filling density of 25% and increases with the filling density. The haze ratio saturates for a filling density higher than 50%. The high haze ratio in the UV–visible regime (300–550 nm) implies a

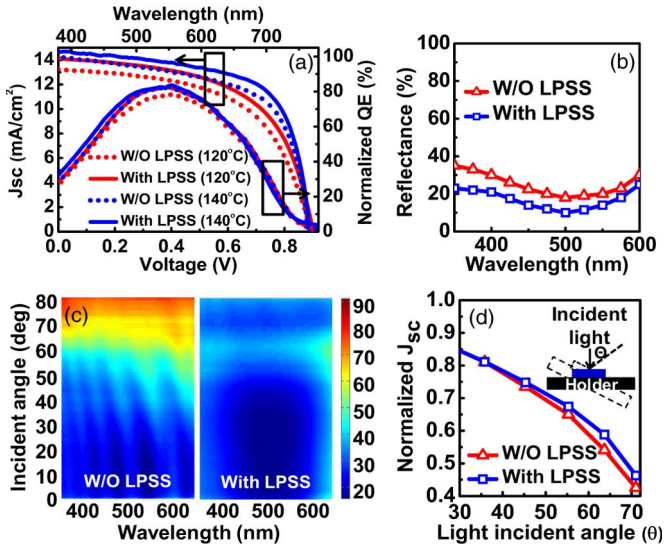

Fig. 3. Photoresponse characteristics of the a-Si SC with (fill density of 65%) and without the LPSS monolayer: (a) I–V and QE spectra of SCs prepared at 120 °C and 140 °C, (b) measured reflectance at normal light incident angle, (c) reflectance distribution map, and (d) measured normalized J_{sc} as a function of the light incident angle. The colored bar in (c) represents the magnitude of the reflectance in percentage.

TABLE I
CELL PERFORMANCES OF THE 120 °C- AND 140 °C-FABRICATED a-SiSCs WITH AND WITHOUT THE LPSS MONOLAYER. THE CELL AREA IS 4 cm^2

	V_{oc} (volt)	J_{sc} (mA/cm^2)	FF (%)	η (%)
W/O LSPP (120 ℃)	0.88	13.33	51.2	6.4
With 50% LSPP (120 ℃)	0.89	14.06	54.0	6.7
With 65% LSPP (120 ℃)	0.90	14.12	57.4	7.3
W/O LSPP (140 ℃)	0.89	14.18	64.1	8.1
With 65% LSPP (140 ℃)	0.89	14.64	65.1	8.5

large light coupling into the a-Si cell as a result of the increase in the optical path in a-Si layer. The large light coupling can enhance light absorption in a-Si; this is in agreement with the simulated results discussed previously.

Fig. 3(a) shows the I–V and QE spectra of the a-Si SCs prepared at 120 °C and 140 °C, and the cell performance is summarized in Table I. The photocurrent of the cell with the LPSS filling density of 65% is significantly enhanced; this can be attributed to a higher QE in the range of 400–550 nm due to the high diffuse transmittance. Furthermore, the LPSS monolayer also enhances conversion efficiency of 120 °C and 140 °C fabricated a-Si SCs to 7.3% and 8.5%, respectively, which are higher than all reported values. The enhancement by LPSS monolayer is about 6.9% and 4.9% on a-Si SCs fabricated at 120 °C and 140 °C, respectively, and confirmed by simulation results and optical characterization.

Moreover, the LPSS monolayer can also reduce the interface reflectance of the a-Si cell as shown in Fig. 3(b), thereby enhancing light absorption and, thus, the J_{sc}. Fig. 3(b) shows that, in the wavelength range of 400–600 nm, the control sample has a reflectance of 20%–35% at the normal incident angle, while the LPSS monolayer clearly reduces the reflectance of the cell by more than 8%. The reflectance reduction is due to the formation of a graded refractive index profile in the LPSS layer. Note that the backside reflector is usually designed to enhance the visible-near-infrared photoresponse of the desired absorption band of a-Si and typically leads to a solar efficiency less than 6.5%. This frontside LPSS design for the UV–visible light trapping apparently outperforms the backside design. The low-temperature fabrication method of a-Si SC with a low-defect density is suitable for flexible SC applications.

In addition to the enhancement in light absorption of the a-Si cell, the LPSS monolayer can also improve the omnidirectional antireflection effect. Fig. 3(c) shows the reflectance distribution map of the a-Si cell as a function of the light incident angle and the wavelength. It can be clearly seen that the light reflectance of the a-Si cell with the LPSS monolayer is greatly reduced at large incident angles for the entire photoresponse band of a-Si SC. As a consequence, the angular reflectance reduction of the LPSS-structured a-Si cell can significantly improve the J_{sc} at different light incident angles as shown in Fig. 3(d). The J_{sc} enhancement due to the LPSS structure becomes clear at the light incident angle larger than 40 °.

IV. CONCLUSION

We have synthesized the LPSS monolayer at room temperature on ICP a-Si SC with a low-defect density. The high conversion efficiency of 8.5% is achieved for the LPSS-structured a-Si cell by optimizing the sphere size and the filling density. Furthermore, the LPSS monolayer results in a nearly omnidirectional antireflection for the a-Si SC, which is particularly effective at a large incident angle. We believe that the low thermal-budget fabrication method of the a-Si SC using the self-assembly LPSS light-trapping structure is a promising technique for flexible SC applications.

REFERENCES

[1] V. E. Ferry, M. A. Verschuuren, H. B. T. Li, E. Verhagen, R. J. Walters, R. E. I. Schropp, H. A. Atwater, and A. Polman, "Light trapping in ultrathin plasmonic solar cells," *Opt. Exp.*, vol. 18, no. S2, pp. A237–A245, Jun. 2010.

[2] J. Zhu, C. M. Hsu, Z. F. Yu, S. H. Fan, and Y. Cui, "Nanodome solar cells with efficient light management and self-cleaning," *Nano Lett.*, vol. 10, no. 6, pp. 1979–1984, Jun. 2010.

[3] P. Matheu, S. H. Lim, D. Derkacs, C. McPheeters, and E. T. Yu, "Metal and dielectric nanoparticle scattering for improved optical absorption in photovoltaic devices," *Appl. Phys. Lett.*, vol. 93, no. 11, pp. 13 108–13 111, Sep. 2008.

[4] Y. A. Akimov, W. S. Koh, S. Y. Sian, and S. Ren, "Nanoparticle enhanced thin film solar cells: Metallic or dielectric nanoparticles?" *Appl. Phys. Lett.*, vol. 93, no. 7, pp. 073111-1–073113-3, Feb. 2010.

[5] M. Kroll, S. Fahr, C. Helgert, C. Rockstuhl, F. Lederer, and T. Pertsch, "Employing dielectric diffractive structures in solar cells—A numerical study," *Phys. Stat. Sol. (A)*, vol. 205, no. 12, pp. 2777–2795, Dec. 2008.

[6] J. Grandidier, D. M. Callahan, J. N. Munday, and H. A. Atwater, "Light absorption enhancement in thin-film solar cells using whispering gallery modes in dielectric nanospheres," *Adv. Mater.*, vol. 23, no. 10, pp. 1272–1276, Mar. 2011.

[7] Y. H. Wang, R. Tummala, L. Chen, L. Q. Guo, W. D. Zhou, and M. Tao, "Solution processed omnidirectional antireflection coatings on amorphous silicon solar cells," *J. Appl. Phys.*, vol. 105, no. 10, pp. 103 501–103 506, May 2009.

[8] C. H. Shen, J. M. Shieh, J. Y. Huang, H. C. Kuo, C. W. Hsu, B. T. Dai, C. T. Lee, C. L. Pan, and F. L. Yang, "Inductively coupled plasma grown semiconductor films for low cost solar cells with improved light-soaking stability," *Appl. Phys. Lett.*, vol. 99, no. 3, pp. 033510-1–033510-3, Jul. 2011.

[9] J. W. Leem, D. H. Joo, and J. S. Yu, "Biomimetic parabola-shaped AZO subwavelength grating structures for efficient antireflection of Si-based solar cells," *Sol. Energy Mater. Sol. Cells*, vol. 95, no. 8, pp. 2221–2227, Aug. 2011.